Investigation of the shock structural formation of the supersonic nozzle jet with longitudinal variation of coaxial pipe location

*SungCheoul Roh, JunYoung Park, and SooYong Kim**
Korea Institute of Machinery & Materials
Thermal Fluid System Department
171 Jan-dong, Yuseong-gu
Daejeon, 305-343, KOREA
sykim@kimm.re.kr

Keywords: Supersonic Jet, Shock Cell Structure, Shadowgraph Visualization, CFD

Abstract

A visualization study of shock formation of the supersonic jet nozzle using a Shadowgraph Method (SM) was carried out to investigate the effect of the longitudinal variation of coaxial pipe end tip position inside the supersonic nozzle. The experiment was performed for the Mach number range from 1.1 to 1.2 at nozzle exit. The well known shock cell structure was shown with the pipe end located deep inside the nozzle for the studied Mach number. With the pipe end approaches nozzle exit, it was found that the shock cell structure disappeared and turned into complex formation. In order to understand the mechanism of the shock structural change, computational simulation was carried out using the Navier-Stokes solver, FLUENT. Topological sketch was added with an aid of the visualization and the numerical simulation.

1. Introduction

In general, the supersonic flow structure ejecting from a cylindrical nozzle has the shape of shock cell and is semi-periodically distributed in the streamwise direction[1)2)3)]. The shock cell flow structure ejected supersonically involves very large noise, and Tam and Jackson[2)] considered that the collision of shock cell appearing semi-periodically with turbulent flow structure rapidly growing downstream jet flow as being the source of the noise. In order to reduce the noise originating from supersonic shock cell flow structure, much study[1)4)5)6)] to procure the revised shock cell flow structure by introducing swirl into the supersonic flow has been carried out. Neemh et al.[5)] showed that the shock cell flow structure is deformed by inclusion of swirl flow from shadowgraph visualization experiments and insisted that the transforming of shock cell flow structure can be an important factor reducing the noise level. Therefore, it is considered very important to understand the shock cell's structural transformation occurring in supersonic nozzle flow.

In the present study, it was attempted to investigate the process of the shock cell flow structure deformation resulting from the movement of a coaxial pipe located inside the supersonic nozzle. For the purpose to understand the deformation process of shock cell flow structure, shadowgraph visualization were employed and a numerical analysis to show the shock cell flow deformation was carried out. Also topological sketches were made to show the deformation of shock cell supersonic flow brought by the existence of coaxial pipe inside a cylindrical nozzle.

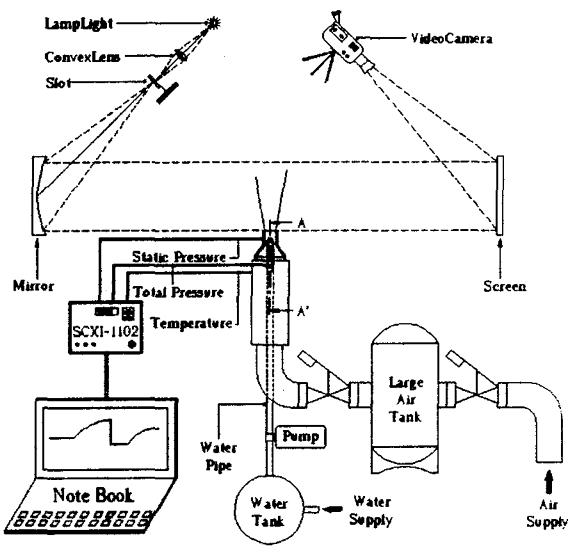

Fig. 1 Schematic of the Experimental Setup

2. Experimental Setup and Numerical Analysis

2.1 Shadow Graph Visualization

Shadowgraph visualization method[7)8)] was employed to see the supersonic flow structure resulting from the movement of a coaxial pipe inside the nozzle and the experimental setup are as shown in Fig. 1. The apparatus to make supersonic flow consists of an air reservoir tank, a pipe for high pressured air flow, and a conical nozzle to eject the flow (Fig. 1). For generating a high pressure air, XA350D compressor of ATLAS COPCO Co., capable of producing $21m^3$/min at 6-7 bar, was used. Experiments were carried out with compressed air of 4 atm, stored in the reservoir. In order to measure the supersonic flow speed, static pressure at nozzle exit and a total pressure inside the pressurized pipe line using a pitot tube were measured (Fig. 2). During experiments, the temperature inside the pipe line remains more or less constant, but shows a slight increase through the repetition of experiment from 25 to 35°C, and therefore, the specific heat is assumed to be constant 1.4. During visualization test, as the pipe end approaches to the nozzle exit, pressure changes before the nozzle throat and exit were measured and Mach number in these cases turned out to be in the range of 1.1 to 1.2.

Shadow graph visualization setup consists of a Xenon lamp for a light source, an electric power supply, two convex lens to transmit light to the flow area, two iris, one concave mirror, and a screen to show images of the density difference in local flow field. The Xenon lamp used in the experiments has 150 watts and the power source to provide electricity to the lamp is required to have a high stability. The concave mirror has a focal distance of 1.6m and diameter of 0.2m, reflects the light from convex lens and iris and then the light become refracted due to a density gradient of supersonic shock wave to be projected to the screen. These flow phenomena appeared in the screen were pictured by a Video camera(GL2, Canon) capable of photographing under low(0.75 lux) light flux condition. The consecutive image of supersonic flow photographed by a video camera was captured instantly (Video Cap Final Plus 200, Digital Video Capture & Editing Board) to give snapshot supersonic flow pictures. Series of flow visualization experiments were carried out at different pipe end positions, x, as shown in Fig 2, where x indicates relative pipe end position from nozzle exit. The experiments made were done at x position of 100, 60 and 53mm. The supersonic nozzle shapes is as shown in Fig. 2, and has an exit diameter of 3.5cm, length 6.0cm, and an inner diameter of 22mm. The pipe inner diameter was 10mm.

2.2 Numerical Analysis

The supersonic jet flow analysis under a comrpessible, steady flow condition was carried out using a commercial software FLUENT. To reduce the time required for the calculation, the flow is assumed to be 2-dimensional, and axi-symmetrical and RNG k-e model was used for the analysis. The 38,000 grid points were generated using the GAMBIT and were evenly distributed for each case. Irrelevant of the inside nozzle positions, inlet flow condition was set to a total pressure of 0.37bar, a total temperature of 300K and the exit to be atmospheric.

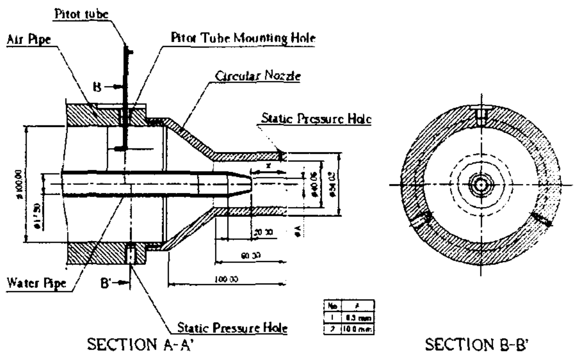

Fig. 2 Circular Nozzle with Coaxial Pipe

3. Results and Discussion

Fig. 3 shows different shapes of shock waves formed at different coaxial pipe end positions inside the nozzle. Fig. 3(a) is a case when the pipe end is located at innermost position (x=100mm), and the overall shock waves in the figure coincide with that of other studies[1)4)5)]. The well known shock cell structure appeared to be semi-periodic pattern as shown in (B) of Fig. 3(a) and confirms the assertion made by Tam and Jackson[2)] and Yu and Chen[4)] that shock cell structure appears semi-periodically in supersonic jet flow. Tam and Jackson[2)] explain the intensity difference noticed in 1st and 2nd cell of Fig. 3(a) such that the turbulence appeared in the mixing area mitigates the sharp speed or density gradient caused by the shock. This type of shock formation rapidly changes due to the relative distance of the coaxial pipe end position to nozzle exit as shown in Fig. 3(b) and (c). That means, as the pipe end approaches nozzle exit (decreasing x), it is noticed that the clear shock cell structure deforms into complicated shock wave structure. Besides, phenomenon of shock wave reflection against the boundary wall by the atmospheric air encompassing the flow is also noticed in Fig. 3.

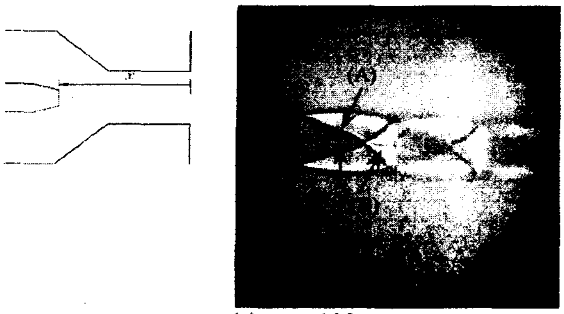

(a) x = 100mm

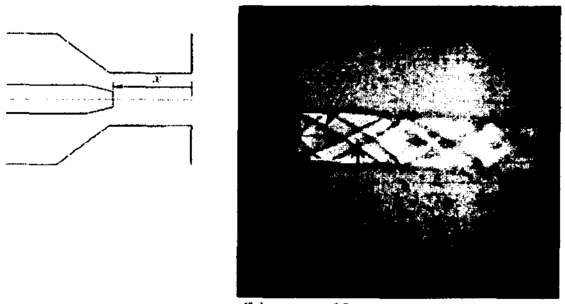

(b) x = 60mm

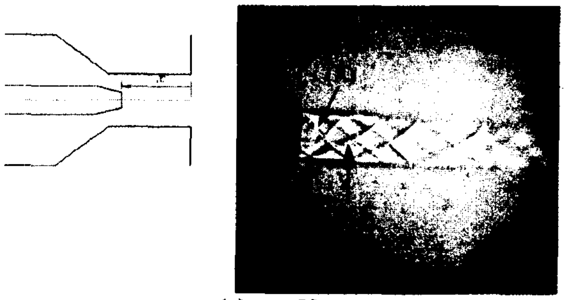

(c) x = 53mm

Fig. 3 Shock Waves from Shadowgraph Visualization

This is considered to be due to a static pressure of the high speed flow being too small compared with an atmospheric pressure, which causes a severe density gradient in the boundary, thereby, the increased density gradient acts as a wall to reflect the shock wave inside the supersonic flow. As noticed in Fig. 3(b), (c), it is considered that rapid deformation of shock wave structure with the coaxial pipe end's approaching toward the nozzle exit is due to the flow structural changes inside the nozzle. Since the nozzle cross section after the throat remains the same (0≤x≤60mm), the flow inside the nozzle will also be considered to be supersonic and forms a complicated flow involving a shock wave depending on the pipe end position. The shock waves created inside the nozzle will make repeated reflection with nozzle wall influencing the shock cell structure outside the nozzle each other and show the phenomena shown in Fig. 3(b), (c). Accordingly, a numerical calculation was executed to characterize the flow structure from the pipe end to the nozzle exit, as a guide to understand the shock cell structural change outside the nozzle exit.

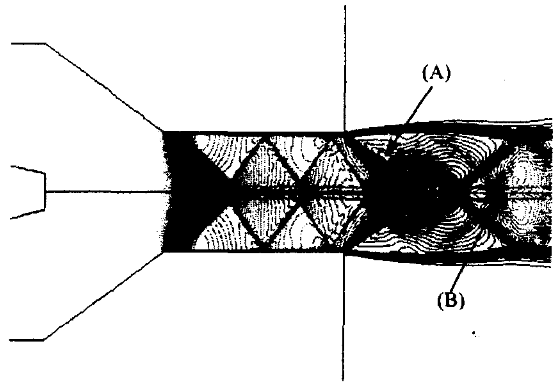

(a) x = 100mm

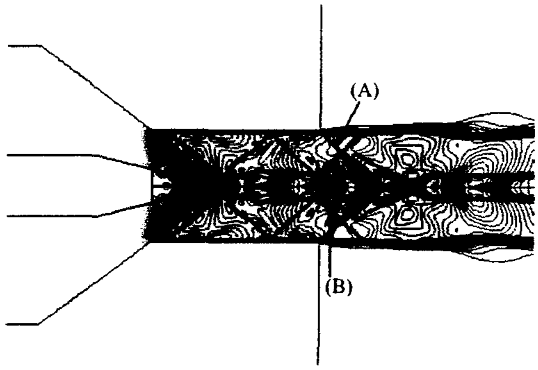

(b) x = 60mm

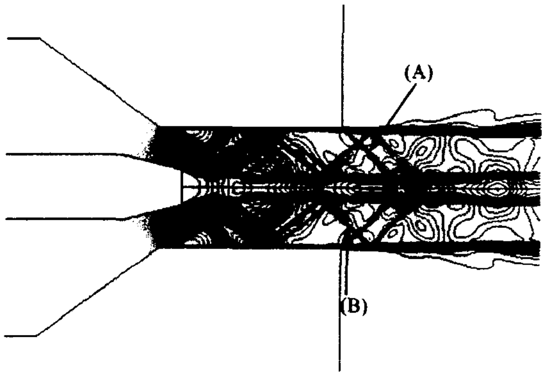

(c) x = 53mm

Fig. 4 Iso-Density Contours from Numerical Simulation

Fig. 4 shows the numerical results of the same cases with the pipe end's positions inside the nozzle as done in visualization tests, and shows density contours for both in and outside of the nozzle. Fig. 4(a) is a case when the pipe end is positioned at innermost position (x=100mm), and it is found that the flow inside the nozzle has not been influenced by the pipe end position and the supersonic flow leaving the nozzle exit forms the well known shock cell formation (compare (A) of Fig. 3(a) and (a) of Fig. 4(a)). The complicated oblique shock formed inside the nozzle shown in Fig. 4(a) is considered to be from the strong incoming flow passing through the nozzle throat. Fig. 4(b) and (c) show the shock wave structure both in and outside the nozzle exit as the pipe end approaches the nozzle exit (Fig. 4(b): x=60mm; Fig. 4(c): x=53mm). As the pipe end approaches the nozzle exit, it is noticed that the pipe end affects directly the flow inside the nozzle and the low speed region from the pipe end extends to the outside region of the nozzle. This type of shock wave, being refracted several times inside the nozzle, takes different flow structure other than the one resulting when the pipe end is located at innermost position(x=100mm). That is, as the pipe end approaches the nozzle exit, the shock wave structure inside the nozzle become more complicated. Comparing Fig. 4(b) and Fig. 4(c), as the pipe end makes shift about 7mm from x=60mm(Fig. 4(b)) to x=53mm (Fig. 4(c)), the shock wave profiles inside the nozzle show some difference such that the shock wave structure seemed to move in the opposite streamwise direction from the flow stream as the pipe end approaches nozzle exit. As a result, the shock wave configuration inside the nozzle influenced by pipe end position seems to have direct effect on the supersonic flow characteristics outside nozzle exit. Comparing shock lines dictated by Fig 3(b) and Fig 4(b), it can be seen that the shock wave visualization results right after the nozzle exit agrees well with the numerical one. Same statement can be made from the comparison of Fig. 3(c) and Fig 4(c). That means shock lines of (A) and (B) in Figs. 3(b), (c) structurally conforms with those of the numerically calculated as shown in Figs. 4(b), (c). Therefore, it is concluded that the drastic deformation of the shock cell structure is directly from the complicated shock waves inside the nozzle and the low speed region after the pipe end. Also, in Fig. 4, it is noticed that highly concentrated density gradients region appears in and outside the central flow region, which coincides with the thin belt indicated by (C) in Figs. 3(a), (b), and (c). From the results of the visualization and the numerical calculation as shown in Fig. 3 and Fig. 4, a topological sketch to illustrate the supersonic shock structural deformation with the coaxial pipe end position change is provided in Fig. 5.

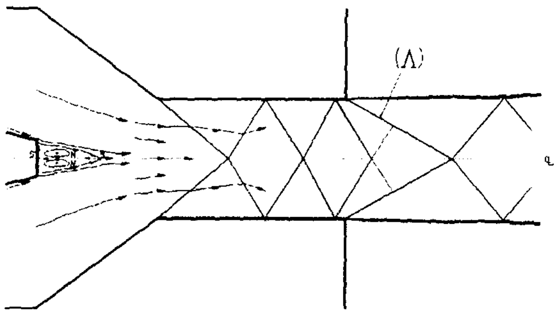

(a) x=100mm

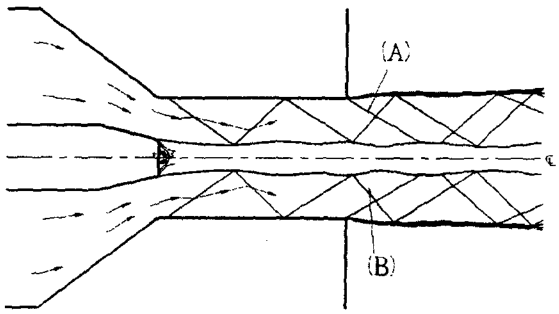

(b) x=60mm

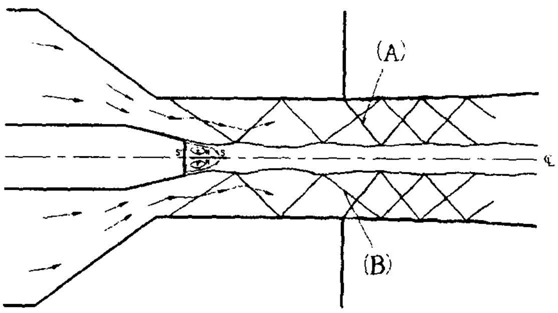

(c) x=53mm

Fig. 5 Topological Sketch

Fig. 5 shows the flow pattern both in and outside the nozzle exit with different pipe end positions. In case the pipe end sit at an innermost position from the nozzle exit, the recirculating flow rising from the pipe end does not affect the flow inside the nozzle, however, as seen in Fig. 5(b) and (c), strong influences of the recirculating flow region and the low speed region after the pipe end are noticed as the pipe end approaches nozzle exit. In Fig 5, N, S, and S' indicate a nodal, a saddle, and a half saddle points, respectively, and these represent the flow characteristics of a two-dimensional cross section.

4. Conclusion

Drastic deformation in shock cell structure outside the circular nozzle with variation of a coaxial pipe end position was confirmed by a shadowgraph visualization method. For the interpretation of such shock cell structural deformation, a numerical analysis was carried out. From the numerical analysis, existence of recirculated flow from the pipe end tip was noticed and revealed that the low speed region rising from the pipe end directly influences the formation of shock waves inside the nozzle. The variation in complicated shock waves inside the nozzle caused by coaxial movements of pipe end position directly affects the shock cell structure outside the nozzle exit and thus forms completely different shock waves. Based on such evidences, topological sketches for the supersonic flow fields in and outside the nozzle and around the coaxial pipe was made.

References

1) R. Smith: An Investigation of Supersonic Swirling Jets, Aeronautical Quarterly, 1973, pp. 167-178.
2) C. K. W. Tam and J. A. Jackson: A Multiple-Scale Model of the Shock-Cell Structure of Imperfectly Expanded Supersonic Jets, J. Fluid Mechanics, Vol. 153, 1985, pp. 123-149.
3) C. K. W. Tam: Supersonic Jet Noise, Annual Review of Fluid Mechanics, Vol. 27, 1995, pp. 17-23.
4) Y. K. Yu and R. H. Chen: A Study of Screech Tone of Supersonic Swirling Jets, Journal of Sound and Vibration, Vol. 205, No. 5, 1997, pp. 698-705.
5) R. Neemeh, S. Algattus, and L. Neemeh: Experimental Investigation of Noise Reduction in Supersonic Jets due to Jet Rotation, Journal of Sound and Vibration, Vol. 221, No. 3, 1999, pp. 505-524.
6) P. W. Carpenter: A Linearized Theory for Swirling Supersonic Jets and Its Application to Shock Cell Noise, AIAA Journal, Vol. 23, 1985, pp. 1902-1909.
7) H. W. Liepman and A. Roshko: Elements of Gas Dynamics, Wiley & Sons, Inc., 1957.
8) R. J. Goldstein: Fluid Mechanics Measurements, Hemisphere Publishing Corporation, 1983.